Domain Walls in Antiferromagnetically Coupled Multilayer Films

Olav Hellwig, Andreas Berger, and Eric E. Fullerton

San Jose Research Center, Hitachi Global Storage Technologies, 650 Harry Road, San Jose, California 95120, USA

(Received 27 May 2003; published 5 November 2003)

We report experimentally observed magnetic domain-wall structures in antiferromagnetically coupled multilayer films with perpendicular anisotropy. Our studies reveal a first-order phase transition from domain walls with no net moment to domain walls with ferromagnetic cores. The transition originates from the competition between dipolar and exchange energies, which we tune by means of layer thickness. Although observed in a synthetic antiferromagnetic system, such domain-wall structures may be expected to occur in *A*-type antiferromagnets with anisotropic exchange coupling.

DOI: 10.1103/PhysRevLett.91.197203 PACS numbers: 75.70.Kw, 75.30.Kz, 75.70.Cn

The study of ferromagnetic materials has been an integral part of modern science and has shaped the progress in a number of important technological fields. Antiferromagnets (AF), on the other hand, are much less understood even though they originate from the same fundamental mechanism, namely, the quantum mechanical exchange interaction [1]. This lack of understanding is well illustrated by the fact that only with the advent of neutron diffraction probes in the early 1950s, the existence and structure of antiferromagnets could be established unambiguously [2]. Our limited knowledge is furthermore responsible, in part, for the limited use of AF materials in technological applications that have only recently emerged in state-of-the-art magnetic read heads [3]. One of the crucial elements for the progress of ferromagnetism as a scientific discipline has been the ability to connect the atomic scale mechanisms with macroscopically and mesoscopically observable properties such as domain and domain-wall structures. A variety of experimental microscopy tools have been developed for this purpose [4]. In almost all cases, one exploits the fact that on mesoscopic length scales ferromagnetic materials exhibit a nonvanishing spin polarization or magnetization and domain structures produce a locally varying flux density B and magnetic field H.

Contrary to the ferromagnetic case, AF materials exhibit a net magnetic moment only on the atomic scale, which renders most magnetic microscopy techniques useless. Only recently have there been a limited number of microscopy studies that allow the characterization of AF domains on the nm scale. Linear x-ray dichroism [5,6] and x-ray microdiffraction [7] have imaged AF domains but do not presently have the resolution to study AF domain walls. Spin-polarized scanning tunneling microscopy was able to detect AF ordering at a Cr crystal surface and image domain-wall-like structures arising from topological defects [8].

A complimentary approach for studying AF thin films is fabricating synthetic AF structures out of thin ferromagnetic films separated by nonmagnetic layers that mediate the AF exchange [9]. For film thickness values below the exchange length, each ferromagnetic layer can be viewed as a macroscopic classical spin and the resulting Hamiltonian is isomorphic to that of a layered AF [10]. This approach has the advantage that the AF periodicity is shifted towards longer length scales, making experimental characterization with more conventional means feasible. Such structures have recently been used to study the fundamental properties of AF materials [10–14]. In this Letter we study the domain and domain-wall structure in AF-coupled multilayers with perpendicular magnetic anisotropy. We observe the occurrence of two classes of domain walls, one with and one without a net ferromagnetic moment, depending on the relative strength of the various energy contributions. Furthermore, we present a microscopic model that explains quantitatively the observed structures.

Co/Pt and Co/Pd multilayers are well-established systems for studying domain structures in ferromagnetic films [15,16]. The break in symmetry at the Co-Pt interface gives rise to perpendicular magnetic anisotropy, and the thin Pt layers couple adjacent Co layers ferromagnetically. By selectively replacing Pt layers with Ru layers of appropriate thickness, adjacent Co layers are AF coupled [14,17]. The resulting structures, $[[\mathrm{Co}(4\ \text{Å})/\mathrm{Pt}(7\ \text{Å})]_{X-1}/\mathrm{Co}(4\ \text{Å})/\mathrm{Ru}(9\ \text{Å})]_N$ multilayers, are made up of N ferromagnetic $[\mathrm{Co/Pt}]_X$ sublayer stacks with perpendicular anisotropy. Each sublayer stack is AF coupled to adjacent sublayer stacks [14]. For sufficiently small values of X and N, the films exhibit an A-type AF ground state with the spins of adjacent Co/Pt blocks aligned antiparallel to each other along the surface normal. Increasing X and N above critical values results in a transition to a ferromagnetic stripe domain ground state [14].

The average magnetic properties were determined by SQUID and magneto-optical Kerr effect magnetometry while the domain structure was characterized by magnetic force microscopy (MFM), x-ray photoelectron emission microscopy (PEEM) [6,18], and transmission x-ray microscopy [19]. The latter two measurements were performed on beam lines 7.3.1.1 and 6.1.2, respectively, at the Advanced Light Source located at the

Lawrence Berkeley National Laboratory. Shown in Fig. 1 is a magnetic hysteresis loop for a sample with $N = 4$ and $X = 7$. There are four discrete steps in the hysteresis loop that correspond to the reversal of each of the four Co/Pt sublayer stacks. The separation in field of each reversal is proportional to the strength of the AF exchange across the Ru interlayer ($J_{ex} = 0.45$ ergs/cm^2) and is given by $J_{ex}/M_S t$ with $M_S = 700$ emu/cm^3 and t being the average magnetization and thickness of a Co/Pt sublayer stack, respectively. The remanent state corresponds to an AF configuration.

After out-of-plane saturation, the sample populates one of the two equaivalent AF configurations (i.e., the magnetization of the four layers pointing down-up down-up vs up-down up-down) and is laterally uniform as shown in inset 1 of Fig. 1. However, after saturating the film with an applied field in the sample plane, we create a remanent state in which both ground states are nearly equally populated froming large AF domains separated by AF domain walls (inset 2 of Fig. 1). The contrast in the MFM images arises from the dipolar fields that are generated by the divergence of the magnetization within the domain walls, whereas the AF domains appear equivalent [20]. The AF domain structure described here is confirmed by combined x-ray microscopy techniques. By virtue of the small electron escape length, PEEM images only the top Co/Pt stack and clear domain contrast is observed with the top Co/Pt stack being magnetized either parallel or antiparallel to the film surface normal. In contrast, transmission x-ray microscopy, which images the magnetic moments averaged over the entire thickness of the film, shows no domain contrast confirming AF domains with no net moment.

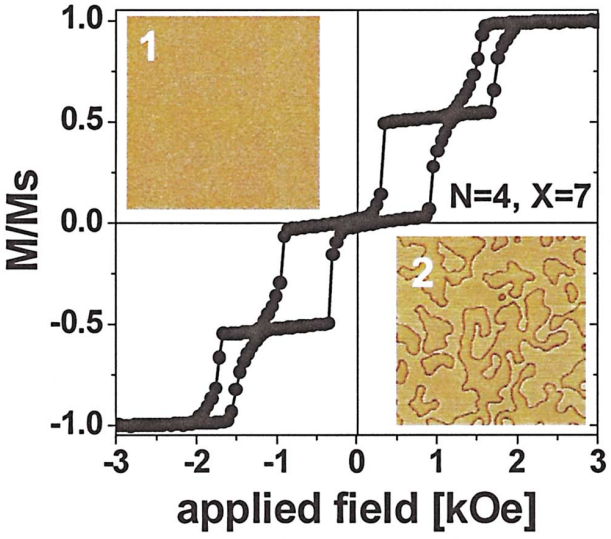

FIG. 1 (color). Magnetic hysteresis loop for a $[[\mathrm{Co}(4\ \text{Å})/\mathrm{Pt}(7\ \text{Å})]_6/\mathrm{Co}(4\ \text{Å})/\mathrm{Ru}(9\ \text{Å})]_4$ multilayer sample with the field applied perpendicular to the film. Inset 1 is an MFM image in remanence after out-of-plane saturation that shows a laterally uniform ground state, while inset 2, measured after in-plane saturation, exhibits domains of the two possible ground states (up-down up-down vs down-up down-up). Both images are $(5\ \mu\mathrm{m})^2$ in size.

For the remainder of the Letter we focus on the nature of the domain walls that separate the two energetically equivalent AF ground states. The five samples we discuss in more detail are ($N = 4, X = 5$), ($N = 4, X = 7$, shown in Fig. 1), ($N = 10, X = 5$), ($N = 12, X = 7$), and ($N = 18, X = 8$). Even though these samples all exhibit AF ground states, the domain walls differ significantly. Shown in Figs. 2(a)–2(d) are MFM images of the samples with dark and bright contrast corresponding to magnetic stray fields parallel and antiparallel to the magnetic probing tip, repsectively. Corresponding line scans across the domain walls for selected samples are shown in Figs. 2(e)–2(g). For the samples with $X = 5$ [Figs. 2(a) and 2(b)], the domain-wall structure appears similar to that described in Ref. [20]. We observe bright and dark contrast across the wall with the magnitudes of the stray

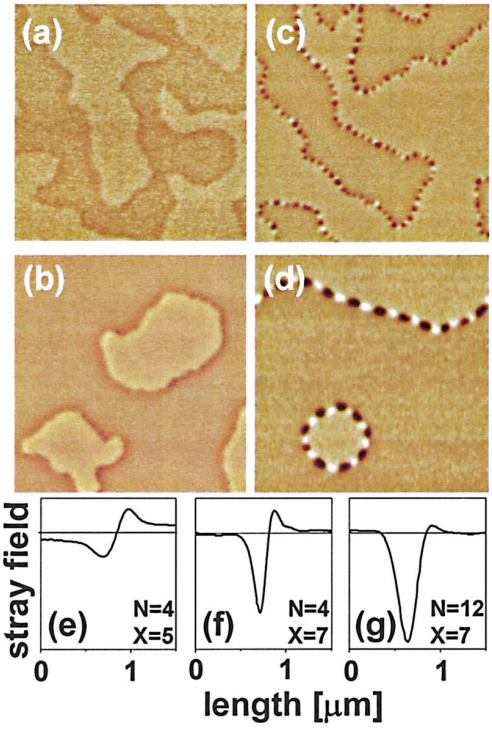

FIG. 2 (color). Details of domain wall structures observed in $[[\mathrm{Co}(4\ \text{Å})/\mathrm{Pt}(7\ \text{Å})]_{X-1}/\mathrm{Co}(4\ \text{Å})/\mathrm{Ru}(9\ \text{Å})]_N$ multilayers. (a)–(d) MFM images where (a) and (c) are $(5\ \mu\mathrm{m})^2$ and (b) and (d) are $(3\ \mu\mathrm{m})^2$ in size. The individual images correspond to the following samples: (a) ($N = 4, X = 5$); (b) ($N = 10, X = 5$); (c) ($N = 12, X = 7$); (d) ($N = 18, X = 8$). (e),(f) MFM line scans across the domain walls for (e) ($N = 4, X = 5$), (f) ($N = 4, X = 7$), and (g) ($N = 12, X = 7$). In order to achieve better statistics, the domain-wall profiles were averaged over a 200–300 nm wide domain-wall region. For the periodic domain-wall patterns only the dark part of the wall was used to determine the profile.

fields being symmetric across the wall [Fig. 2(e)]. This type of profile is characteristic of an AF domain wall with no net moment. We can view each Co/Pt sublayer stack as having a ferromagnetic domain wall. If the domain walls of each sublayer align vertically, then the AF exchange energy is minimized and the domain wall of the composite structure carries no net magnetic moment.

In contrast, the domain walls for the $X = 7$ and $X = 8$ samples [Figs. 1, 2(c), and 2(d)] appear in MFM images as a dark band or exhibit periodic light and dark contrast along the domain walls. The corresponding stray field profiles [Figs. 2(f) and 2(g)] exhibit a nonvanishing integrated signal, which suggests that the domain walls possess a net moment. Such a ferromagnetic structure could naturally originate by shifting the domain walls within each Co/Pt sublayer relative to the neighboring sublayers as shown schematically in Fig. 3(a). Shifting the domains in adjacent layers thus creates a ferromagnetic stripe of width d, in which the magnetization of each layer is aligned parallel. The creation of the ferromagnetic region is driven by the dipolar interactions between adjacent sublayers but comes at the expense of the AF exchange energy. Furthermore, the overall dipolar fields generated by such a ferromagnetic domain wall can be reduced by having the orientation of the ferromagnetic regions reverse periodically along the domain wall (by alternating the relative shift of the individual layer domain walls). This produces the periodic domain-wall structure seen in Figs. 2(c) and 2(d) and is the one-dimensional equivalent of periodic stripe domains that form in ferromagnetic thin films with perpendicular anisotropy [21]. Similar structures are observed for Néel walls in thin ferromagnetic films with in-plane anisotropy [4].

To test the validity of the above-described physical picture we have calculated the total energy of such antiferromagnetic domain walls as a function of the shift d. The energy was calculated using a "quasi"-one-dimensional model, in which the domain wall in each individual ferromagnetic layer was assumed to be a Bloch-type wall of fixed width, which we estimated to be 7.3 nm for our samples based on the measured anisotropy and assuming metallic exchange [14]. The domain walls of the individual layers were then stacked along the thickness of the film, while allowing for an alternating position shift d in between adjacent layers to minimize its total energy. Because the change in dipolar energy due to the shift d is localized in the ferromagnetic core of the domain wall, the energy of this structure can be calculated in a straightforward fashion. A finite size grid calculation using the La Bonte's interaction matrix method allows for an efficient calculation of the total energy change, including interlayer exchange and dipolar contributions [22].

Figure 3(b) shows a contour plot of the total energy relative to the $d = 0$ case as a function of the shift d and

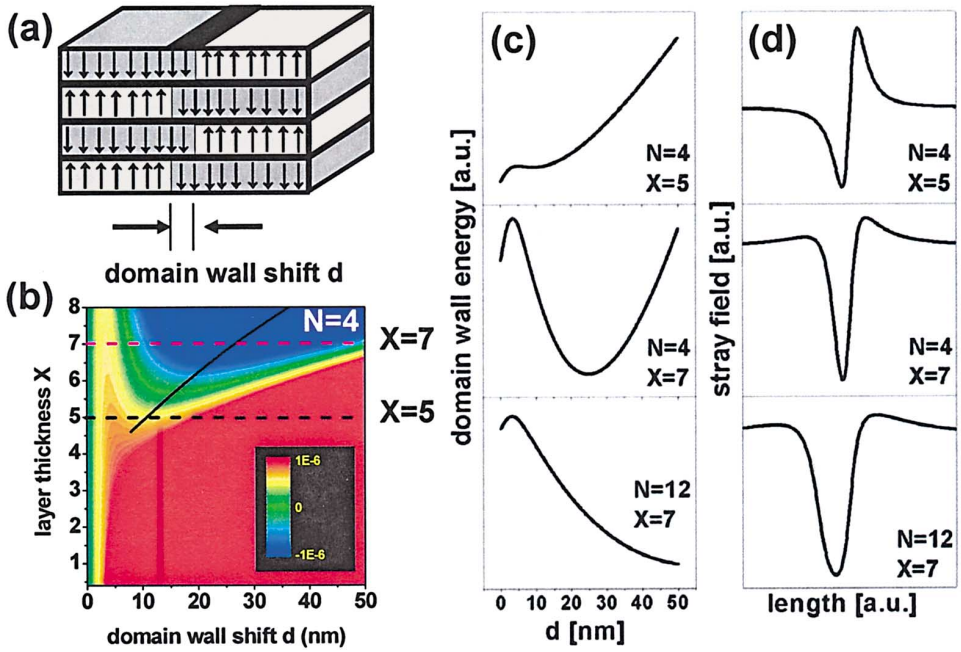

FIG. 3 (color). (a) Schematic illustration of the underlying magnetic domain-wall structure in the AF-coupled multilayers with finite shift d. (b) Contour plot of the calculated AF domain-wall energy versus layer thickness and domain-wall shift d for $N = 4$. The energy is plotted relative to the energy for $d = 0$. The horizontal cuts through the contour plots [marked by the dashed lined and labeled ($X = 5$) and ($X = 7$)] correspond to the first two energy profiles shown in (c). The solid line corresponds to the d value that gives the lowest energy. (c) Energy versus domain wall shift d for three different samples. (d) Calculated magnetic stray field profiles above the film across the equilibrium domain wall structure determined from the minimum in (c).

the layer thickness X for the case $N = 4$. Equivalent calculations for larger N values exhibit qualitatively similar behavior. For thin Co/Pt sublayer thicknesses ($X \lesssim 5$) we find that $d = 0$ is the lowest energy state. However, as one increases X, a second minimum appears at an intermediate d value. The energy of this secondary minimum decreases with increasing sublayer thickness, making it the global minimum for $X > 5.7$. The two energy minima can be more clearly seen by plotting the total energy versus d for fixed layer thickness. Such plots are shown in Fig. 3(c) for layer thickness values corresponding to three of our samples. Consistent with our experimental observation, the model predicts the aligned wall to be stable for the $X = 5$ samples. Furthermore, the calculations in Fig. 3(c) show that both the aligned wall and the shifted domain-wall configurations remain as local minima through the transition suggesting that the transition is first order.

Shown in Fig. 3(d) are the calculated stray field profiles expected for the equilibrium domain-wall structures. For $N = 4$, $X = 5$ we find $d = 0$ while for $N = 4$, $X = 7$ and $N = 12$, $X = 7$, d is estimated to be 26.7 nm and 60.3 nm, respectively. Comparing the theoretical profiles with our experimental observation [Figs. 2(e)–2(g)] we obtain excellent agreement. The theoretically derived stray field profiles confirm the transition from a symmetric to an asymmetric stray field profile due to the formation of a ferromagnetic core within the domain-wall structure.

In conclusion, we have studied the domain-wall structure of AF-coupled multilayer films with perpendicular anisotropy which may be viewed as a model system for A-type AF materials. We observe a phase transition from nonmagnetic to ferromagnetic domain walls with increasing film thickness. The transition originates from the competition between dipolar and exchange energy, which we were able to tune by means of the individual sublayer thickness or total film thickness. Similar results are obtained by tuning the interlayer exchange coupling or the moment density. While such ferromagnetic domain-wall structures are not expected to occur in antiferromagnets where the exchange coupling dominates all secondary interactions (e.g., MnF_2), they may occur in A-type antiferromagnets, which exhibit anisotropic exchange coupling [23]. This class of materials includes many of the Ruddlesden-Popper series of perovskites including the manganites, cobaltites, and nickelates where naturally layered $La_{1.4}Sr_{1.6}Mn_2O_7$ is an example [24]. In such systems mesoscopic domain structures and separation of AF and FM phases are observed and may, in fact, be an intrinsic property of these materials [25]. While we studied the ground state behavior, AF domain walls containing a ferromagnetic core could also be stabilized in an applied field where AF materials with domains would exhibit novel field dependent behavior compared to single-domain materials.

We are indebted to Greg Denbeaux and Andrew Doran for their assistance. O. H. was partially supported by the Deutsche Forschungsgemeinschaft via a Forschungsstipendium under Contract No. HE 3286/2-1.

[1] W. Heisenberg, Z. Phys. **49**, 619 (1928).
[2] C. G. Shull, W. A. Strauser, and E. O. Wollan, Phys. Rev. **83**, 333 (1951).
[3] J. C. S. Kools, IEEE Trans. Magn. **32**, 3165 (1996).
[4] A. Hubert and R. Schäfer, *Magnetic Domains* (Springer-Verlag, Berlin, 1998).
[5] A. Scholl *et al.*, Science **287**, 1014 (2000).
[6] F. Nolting *et al.*, Nature (London) **405**, 767 (2000).
[7] P. G. Evans *et al.*, Science **295**, 1042 (2002).
[8] M. Kleiber *et al.*, Phys. Rev. Lett. **85**, 4606 (2000).
[9] P. Grünberg *et al.*, Phys. Rev. Lett. **57**, 2442 (1986).
[10] R. W. Wang *et al.*, Phys. Rev. Lett. **72**, 920 (1994).
[11] S. G. E. te Velthuis *et al.*, Phys. Rev. Lett. **89**, 127203 (2002).
[12] J.S. Jiang *et al.*, Phys. Rev. B **61**, 9653 (2000).
[13] D. L. Nagy *et al.*, Phys. Rev. Lett. **88**, 157202 (2002).
[14] O. Hellwig *et al.*, Nat. Mater. **2**, 112 (2003).
[15] P. F. Garcia *et al.*, Appl. Phys. Lett. **47**, 178 (1985).
[16] M. T. Johnson *et al.*, Rep. Prog. Phys. **59**, 1409–1458 (1996).
[17] M. M. H. Willekens *et al.*, in *Magnetic Ultrathin Films: Multilayers and Surfaces, Interfaces and Characterization*, edited by B.T. Jonker *et al.*, MRS Symposia Proceedings No. 313 (Materials Research Society, Pittsburgh, 1993), p. 129.
[18] S. Anders *et al.*, Rev. Sci. Instrum. **70**, 3973 (1999).
[19] P. Fischer *et al.*, IEEE Trans. Magn. **38**, 2427 (2002).
[20] S. Hamada *et al.*, J. Magn. Magn. Mater. **240**, 539 (2002).
[21] C. Kittel, Phys. Rev. **70**, 965 (1946).
[22] A. E. La Bonte, J. Appl. Phys. **40**, 2450 (1969).
[23] L. J. de Jongh and A. R. Miedema, Adv. Phys. **50**, 947 (2001).
[24] U. Welp *et al.*, Phys. Rev. Lett. **83**, 4180 (1999).
[25] E. Dagotto, T. Hotta, and A. Moreo, Phys. Rep. **344**, 1 (2001).